

# Human hematopoietic stem/progenitor cells modified by zinc-finger nucleases targeted to *CCR5* control HIV-1 *in vivo*

Nathalia Holt<sup>1</sup>, Jianbin Wang<sup>2</sup>, Kenneth Kim<sup>2</sup>, Geoffrey Friedman<sup>2</sup>, Xingchao Wang<sup>3</sup>, Vanessa Taupin<sup>3</sup>, Gay M Crooks<sup>4</sup>, Donald B Kohn<sup>4</sup>, Philip D Gregory<sup>2</sup>, Michael C Holmes<sup>2</sup> & Paula M Cannon<sup>1</sup>

**CCR5 is the major HIV-1 co-receptor, and individuals homozygous for a 32-bp deletion in *CCR5* are resistant to infection by CCR5-tropic HIV-1. Using engineered zinc-finger nucleases (ZFNs), we disrupted *CCR5* in human CD34<sup>+</sup> hematopoietic stem/progenitor cells (HSPCs) at a mean frequency of 17% of the total alleles in a population. This procedure produces both mono- and bi-allelically disrupted cells. ZFN-treated HSPCs retained the ability to engraft NOD/SCID/IL2 $\gamma$ <sup>null</sup> mice and gave rise to polyclonal multi-lineage progeny in which *CCR5* was permanently disrupted. Control mice receiving untreated HSPCs and challenged with CCR5-tropic HIV-1 showed profound CD4<sup>+</sup> T-cell loss. In contrast, mice transplanted with ZFN-modified HSPCs underwent rapid selection for *CCR5*<sup>-/-</sup> cells, had significantly lower HIV-1 levels and preserved human cells throughout their tissues. The demonstration that a minority of *CCR5*<sup>-/-</sup> HSPCs can populate an infected animal with HIV-1-resistant, *CCR5*<sup>-/-</sup> progeny supports the use of ZFN-modified autologous hematopoietic stem cells as a clinical approach to treating HIV-1.**

The entry of HIV-1 into target cells involves sequential binding of the viral gp120 Env protein to the CD4 receptor and a chemokine co-receptor<sup>1</sup>. CCR5 is the major co-receptor used by HIV-1 and is expressed on key T-cell subsets that are depleted during HIV-1 infection, including memory T cells<sup>2</sup>. A genetic 32-bp deletion in *CCR5* (*CCR5* $\Delta$ 32) is relatively common in Western European populations and confers resistance to HIV-1 infection and AIDS in homozygotes<sup>3,4</sup>. The absence of any other significant phenotype associated with a lack of CCR5 (refs. 5–7) has spurred the development of therapies aimed at blocking the virus–CCR5 interaction, and CCR5 antagonists have proved to be an effective salvage therapy in patients with drug-resistant strains of HIV-1 (ref. 8).

Recently, the ability of *CCR5*<sup>-/-</sup> mobilized CD34<sup>+</sup> peripheral blood cells to generate HIV-resistant progeny that suppress HIV-1 replication *in vivo* was demonstrated in an HIV-infected patient undergoing transplantation from a homozygous *CCR5* $\Delta$ 32 donor during treatment for acute myeloid leukemia<sup>9</sup>. The donor cells conferred long-term control of HIV-1 replication and restored the patient's CD4<sup>+</sup> T-cell levels in the absence of antiretroviral drug therapy. These clinical data support the potential of gene or stem cell therapies based on the elimination of CCR5. However, the risks associated with allogeneic transplantation and the impracticality of obtaining sufficient numbers of matched *CCR5* $\Delta$ 32 donors<sup>10</sup> mean that broader application of this approach will require methods for generating autologous *CCR5*<sup>-/-</sup> cells. Various gene therapy approaches to block *CCR5* expression are being evaluated, including *CCR5*-specific ribozymes<sup>11,12</sup>, siRNAs<sup>13</sup> and intrabodies<sup>14</sup>. The targeted cell populations

include both mature T cells and CD34<sup>+</sup> HSPCs. Loss of *CCR5* in HSPCs appears to have no adverse effects on hematopoiesis<sup>12,13,15</sup>.

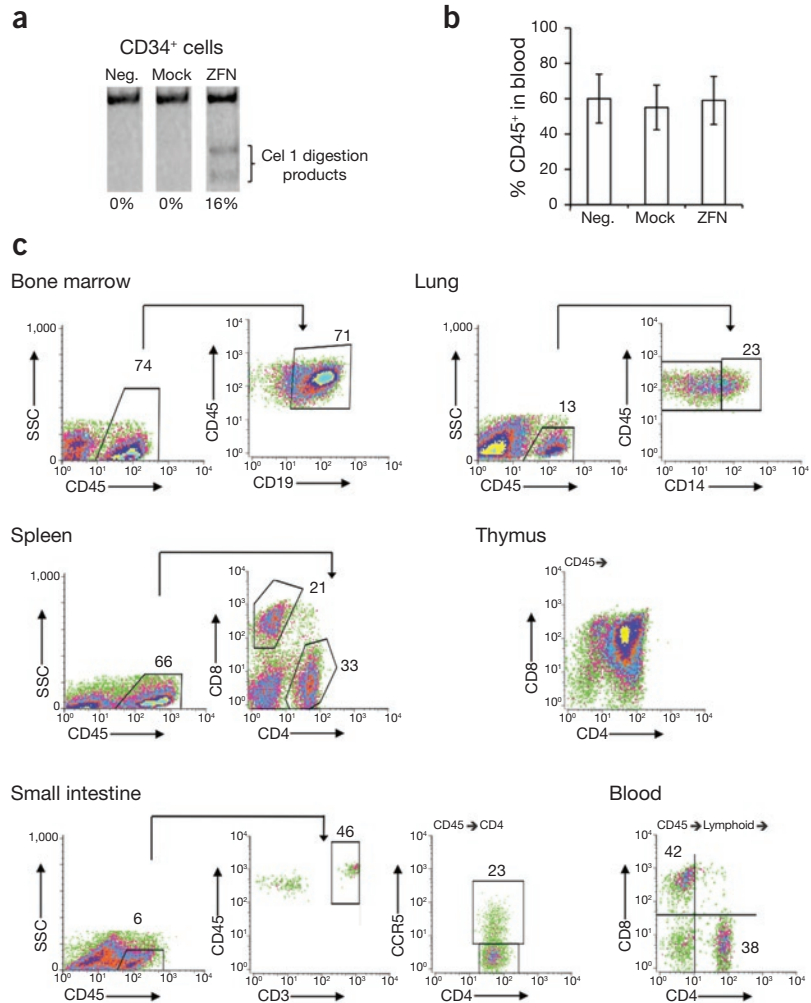
An alternative approach is the use of engineered ZFNs to permanently disrupt the *CCR5* open reading frame. ZFNs comprise a series of linked zinc fingers engineered to bind specific DNA sequences and fused to an endonuclease domain<sup>16</sup>. Concerted binding of two juxtaposed ZFNs on DNA, followed by dimerization of the endonuclease domains, generates a double-stranded break at the DNA target. Such double-stranded breaks are rapidly repaired by cellular repair pathways, notably the mutagenic nonhomologous end-joining pathway, which leads to frequent disruption of the gene due to the addition or deletion of nucleotides at the break site<sup>17,18</sup>. A significant advantage of this approach is that permanent gene disruption can result from only transient ZFN expression.

CD4<sup>+</sup> T cells modified by *CCR5*-targeted ZFNs<sup>19</sup> are currently being evaluated in a clinical trial. However, disruption of *CCR5* in HSPCs is likely to provide a more durable anti-viral effect and to give rise to *CCR5*<sup>-/-</sup> cells in both the lymphoid and myeloid compartments that HIV-1 infects. To evaluate this approach, we optimized the delivery of *CCR5*-specific ZFNs to human CD34<sup>+</sup> HSPCs and transplanted the modified cells into nonobese diabetic/severe combined immunodeficient/interleukin 2 $\gamma$ <sup>null</sup> (NOD/SCID/IL2 $\gamma$ <sup>null</sup>, NSG) mice, which support both human hematopoiesis<sup>20</sup> and HIV-1 infection<sup>13</sup>. Infection of the mice with a *CCR5*-tropic strain of HIV-1 led to rapid selection for *CCR5*<sup>-</sup> human cells, a significant reduction in viral load and protection of human T-cell populations in the key tissues that HIV-1 infects. These

<sup>1</sup>Keck School of Medicine of the University of Southern California, Los Angeles, California, USA. <sup>2</sup>Sangamo BioSciences, Inc., Richmond, California, USA. <sup>3</sup>Childrens Hospital Los Angeles, Los Angeles, California, USA. <sup>4</sup>David Geffen School of Medicine at the University of California Los Angeles, Los Angeles, California, USA. Correspondence should be addressed to P.M.C. (pcannon@usc.edu).

Received 20 October 2009; accepted 24 June 2010; published online 2 July 2010; doi:10.1038/nbt.1663

**Figure 1** ZFN-mediated disruption of *CCR5* in  $CD34^+$  HSPCs. **(a)** Representative gel showing extent of *CCR5* disruption in  $CD34^+$  HSPCs 24 h after nucleofection with ZFN-expressing plasmids (ZFN) or mock nucleofected (mock). Neg. is untreated  $CD34^+$  HSPCs. *CCR5* disruption was measured by PCR amplification across the ZFN target site, followed by Cel 1 nuclease digestion and quantification of products by PAGE. **(b)** Graph showing mean  $\pm$  s.d. percentage of human  $CD45^+$  cells in peripheral blood of mice at 8 weeks after transplantation with either untreated, mock nucleofected or ZFN nucleofected  $CD34^+$  HSPCs ( $n = 5$  each group). **(c)** FACS profiles of human cells from various organs of one representative mouse into which ZFN-treated  $CD34^+$  HSPCs were transplanted. Cells were gated on FSC/SSC (forward scatter/ side scatter) to remove debris. Staining for human  $CD45$ , a pan leukocyte marker, was used to reveal the level of engraftment with human cells in each organ.  $CD45^+$ -gated populations were further analyzed for subsets, as indicated:  $CD19$  (B cells) in bone marrow,  $CD14$  (monocytes/macrophages) in lung,  $CD4$  and  $CD8$  (T cells) in thymus and spleen and  $CD3$  (T cells) in the small intestine (lamina propria). The  $CD45^+$  population from the small intestine was further analyzed for  $CD4$  and *CCR5* expression. Peripheral blood cells from  $CD45^+$  and lymphoid gates were analyzed for  $CD4$  and  $CD8$  expression. The percentage of cells in each indicated area is shown. No staining was observed with isotype-matched control antibodies (**Supplementary Fig. 1**) or in animals receiving no human graft (data not shown).



findings suggest that ZFN engineering of autologous HSPCs may enable long-term control of HIV-1 in infected individuals.

## RESULTS

### Efficient disruption of *CCR5* in human $CD34^+$ HSPCs

Gene delivery methods suitable to express ZFNs include plasmid DNA nucleofection<sup>16</sup>, integrase-defective lentiviral vectors<sup>21</sup> and adenoviral vectors<sup>19</sup>. Although nonviral methods are attractive, nucleofection can be associated with relatively high toxicity for human  $CD34^+$  HSPCs and loss of engraftment potential<sup>22</sup>, although, more recently, less toxic outcomes have been described<sup>23–25</sup>. We evaluated different parameters to identify nucleofection conditions that allowed efficient disruption of *CCR5* while limiting toxicity. The extent of *CCR5* disruption was quantified using PCR amplification across the *CCR5* locus, denaturation and reannealing of products, and digestion with the Cel 1 nuclease, which preferentially cleaves DNA at distorted duplexes caused by mismatches. The Cel 1 nuclease assay detects a linear range of *CCR5* disruption between 0.69% and 44% of the total alleles in a population, with an upper limit of sensitivity of 70–80% disruption (ref. 19 and data not shown). We used this assay to monitor *CCR5* disruption as only a minority of human  $CD34^+$  cells expresses *CCR5* (ref. 26), making it difficult to measure *CCR5* expression by flow cytometry.

Using  $CD34^+$  HSPCs harvested from umbilical cord blood and optimized nucleofection conditions, we achieved mean disruption rates of

17%  $\pm$  10 ( $n = 21$ ) of the total *CCR5* alleles in the population (**Fig. 1a**). Similar results were also achieved using  $CD34^+$  HSPCs isolated from human fetal liver (data not shown). Previous studies in human cell lines<sup>16</sup> and primary human T cells<sup>19</sup> have shown that the percentage of bi-allelically modified cells in a ZFN-treated population is 30–40% of the total number of disrupted alleles detected by the Cel 1 assay. We therefore estimated that 5–7% of ZFN-treated cells would be *CCR5*<sup>-/-</sup>, although this was not directly measured.

We evaluated toxicity by measuring induction of apoptosis. Although nucleofection increased toxicity to human  $CD34^+$  cells threefold compared to untreated cells, inclusion of the ZFN plasmids had no additional effect compared to mock nucleofected controls (data not shown). Overall, we consider that any adverse effects of nucleofection on cell viability may be offset by the high levels of *CCR5* disruption achieved as well as the speed and simplicity of the procedure compared to viral vector systems<sup>19,21</sup>.

### ZFN-modified $CD34^+$ HSPCs are capable of multi-lineage engraftment in NSG mice

NSG mice can be engrafted with human  $CD34^+$  HSPCs<sup>20</sup> and thereby provide a rigorous readout of the hematopoietic potential of genetically modified HSPCs. We evaluated the effects of nucleofection and/or *CCR5* disruption by transplanting both untreated and ZFN-treated human  $CD34^+$  HSPCs into 1-d-old mice that had received low-dose (150 cGy) radiation. Engraftment of human cells was efficient and rapid,

typically resulting in 40% human CD45<sup>+</sup> leukocytes in the peripheral blood at 8 weeks after transplantation. The animals showed no obvious toxicity or ill health, as reported for higher radiation doses<sup>27</sup>. ZFN-treated cells engrafted NSG mice as efficiently as untreated control cells (**Fig. 1b**), with no statistically significant difference between the two groups (Student's *t*-test, *P* = 0.26).

Eight to 12 weeks after transplantation, we analyzed engraftment of various mouse tissues with human CD45<sup>+</sup> leukocytes and with cells from specific hematopoietic lineages (**Fig. 1c**). Human cells were detected using human-specific antibodies, and specificity was confirmed using both unengrafted animals and isotype-matched antibody controls (**Supplementary Fig. 1**). High levels of human cells were found in both the peripheral blood and tissues, ranging from 5–15% of the intestine, >50% of blood, spleen and bone marrow, and >90% of the thymus (**Supplementary Table 1**). CD4<sup>+</sup> and CD8<sup>+</sup> T cells were present in multiple organs, including the thymus, spleen, and both the intraepithelial and lamina propria regions of the small and large intestines; B-cell progenitors were present in the bone marrow; and CD14<sup>+</sup> macrophage and/or monocytes were detected in the lung. Of particular interest was the large population of human CD4<sup>+</sup>CCR5<sup>+</sup> cells in the intestines, as these cells are targeted by both HIV-1 in humans<sup>28–31</sup> and SIV in primates<sup>32–34</sup>. Overall, the profile of human cells in mice receiving ZFN-treated CD34<sup>+</sup> HSPCs was indistinguishable from that of mice transplanted with unmodified cells, both with respect to the percentage of human cells in each tissue and the frequencies of different subsets (**Supplementary Table 1**), suggesting that ZFN-modified CD34<sup>+</sup> HSPCs are functionally normal.

### ZFN-treated CD34<sup>+</sup> HSPCs produce CCR5-disrupted progeny after secondary transplantation

To evaluate whether ZFN treatment of the bulk CD34<sup>+</sup> population modified true SCID-repopulating stem cells, we harvested bone marrow from an animal 18 weeks after engraftment with ZFN-treated CD34<sup>+</sup> HSPCs, in which the extent of CCR5 disruption in the bone marrow was 11% (**Table 1**). This marrow was transplanted into three 8-week-old recipients. At the same time, bone marrow from a control animal engrafted with

**Table 1** Secondary transplantation of ZFN-treated HSPCs

Donor animals <sup>a</sup>	CD45 <sup>b</sup> blood (%)	Cel 1 <sup>c</sup> BM (%)	Secondary recipients	CD45 <sup>b</sup> blood (%)	Cel 1 <sup>c</sup> blood (%)
ZFN (1)	41	11	ZFN (3)	34 +/- 5	16 +/- 4
Neg. (1)	47	0	Neg. (3)	37 +/- 7	0 +/- 0

<sup>a</sup>Bone marrow (BM) was harvested from donor mice engrafted with ZFN-treated HSPCs (ZFN) or untreated HSPCs (Neg.) and transplanted into three secondary recipients for each BM. <sup>b</sup>Levels of human CD45<sup>+</sup> cells were measured in blood of both donor and recipient mice at 8 weeks post-transplantation. <sup>c</sup>CCR5 disruption rates, measured by Cel 1 analysis of donor BM at time of harvest and in blood of recipient mice at 10 weeks post-transplantation.

untreated CD34<sup>+</sup> HSPCs was transplanted into three additional animals. Analysis of the peripheral blood of the secondary recipients 8 weeks later revealed that all six animals had engrafted and that there was no significant difference in the percentage of human CD45<sup>+</sup> leukocytes between the ZFN-treated and control groups. Furthermore, human cells in the blood of the ZFN cohort had levels of CCR5 disruption that slightly exceeded the level in the original donor marrow (12–20%) (**Table 1**). These data demonstrate that ZFN activity can lead to permanent disruption of CCR5 in SCID-repopulating stem cells and that such modified cells retain their engraftment and differentiation potential.

### Protection of CD4<sup>+</sup> T cells in peripheral blood of NSG mice after HIV-1 infection

Engrafted animals at 8–12 weeks after transplantation that had received either unmodified or ZFN-treated CD34<sup>+</sup> HSPCs were challenged with the CCR5-tropic virus HIV-1<sub>BAL</sub>. This strain of HIV-1 causes a robust infection and significant CD4<sup>+</sup> T-cell depletion in humanized mouse models<sup>35,36</sup>, mimicking the human infection, in which depletion of CD4<sup>+</sup>CCR5<sup>+</sup> lymphocytes results from a combination of direct infection, systemic immune activation<sup>36</sup> and the upregulation of CCR5 on thymic precursors<sup>37,38</sup>. After infection, blood samples were collected from the mice every 2 weeks and analyzed for HIV-1 RNA levels, T-cell subsets and the extent of CCR5 disruption. At 8–12 weeks after infection, animals were euthanized and multiple tissues analyzed (**Supplementary Fig. 2**).

Changes in the ratio of CD4<sup>+</sup> to CD8<sup>+</sup> T cells in the peripheral blood are characteristic of progressive infection in individuals with AIDS<sup>39,40</sup>. We therefore examined the CD4/CD8 ratio in blood samples from individual mice both before and after infection and found that the mean ratio before infection was similar for both the untreated and ZFN-treated

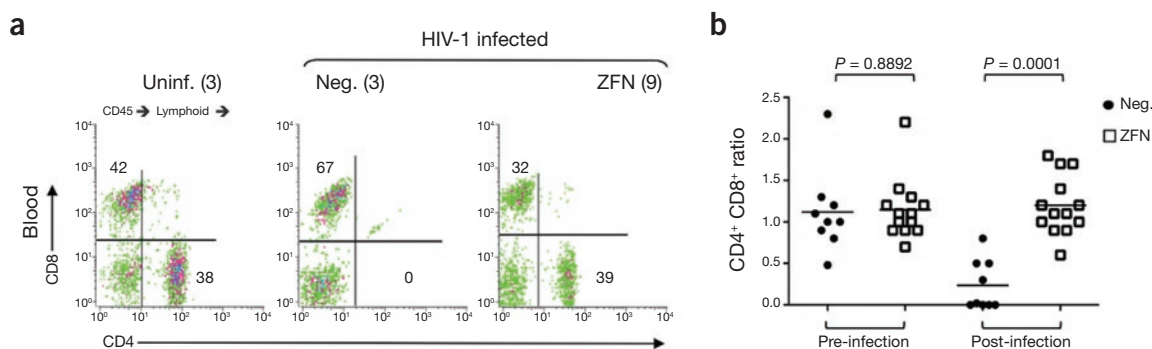


**Figure 2** Protection of human CD4<sup>+</sup> T cells in peripheral blood of HIV-infected mice previously engrafted with ZFN-modified CD34<sup>+</sup> HSPCs. **(a)** FACS plots showing human CD4<sup>+</sup> and CD8<sup>+</sup> T cells in peripheral blood of representative animals from each of three cohorts: uninfected mice previously engrafted with either untreated or ZFN-treated CD34<sup>+</sup> HSPCs (Uninf.), and HIV-1 infected animals previously engrafted with either untreated (Neg.) or ZFN-treated (ZFN) CD34<sup>+</sup> HSPCs, at 4 weeks post-infection. The total number of animals analyzed in each cohort is indicated. Cells were gated on FSC/SSC to remove debris, on human CD45, and a lymphoid gate applied. Percentage of cells in indicated compartments is shown. **(b)** Ratio of human CD4<sup>+</sup> to CD8<sup>+</sup> lymphocytes in peripheral blood of individual mice into which untreated (Neg.) or ZFN-modified CD34<sup>+</sup> HSPCs were transplanted, measured pre-infection and at 6–8 weeks post-infection. Statistical analysis comparing Neg. and ZFN cohorts at each time point is shown.



groups. After HIV-1 challenge, the ratios became highly skewed in the control group owing to the pronounced loss of CD4<sup>+</sup> cells, whereas the ZFN-treated animals maintained normal ratios (Fig. 2a,b).

### Protection of human cells in mouse tissues after HIV-1 infection

We next analyzed the human cells present in various mouse tissues 12 weeks after infection with HIV-1<sub>BAL</sub>. NSG mice into which unmodified cells were transplanted displayed a characteristic loss of certain human cell populations, whereas the ZFN-treated cohort retained normal human cell profiles throughout their tissues despite HIV-1 challenge (Fig. 3a). In the intestines and spleen, which are the organs harboring the highest percentage of human CD4<sup>+</sup>CCR5<sup>+</sup> cells in this model (Supplementary Fig. 3), we observed specific depletion

of CD4<sup>+</sup> T cells from the spleen and the complete loss of all human lymphocytes from the intestines of untreated animals, whereas these populations were fully preserved in the ZFN-treated cohort (Fig. 3b). In the bone marrow, which is not a major target organ of HIV-1 infection, levels of human CD45<sup>+</sup> cells were similar in all three groups.

Notably, HIV-1<sub>BAL</sub> infection resulted in the loss of virtually all human cells from the thymus of mice receiving untreated CD34<sup>+</sup> HSPCs by 12 weeks after infection (Fig. 3a). Depletion of thymocytes has been proposed to occur as a consequence of the upregulation of CCR5 on these cells during HIV-1 infection<sup>37,38</sup>, and likely contributed both to the observed depletion in the thymus and to the reduction in the numbers of mature CD4<sup>+</sup> and CD8<sup>+</sup> T cells observed in other tissues.

### HIV-1 infection rapidly selects for CCR5<sup>-</sup> T cells

We examined whether the survival of T cells in the mice receiving ZFN-treated CD34<sup>+</sup> HSPCs was the result of selection for ZFN-modified progeny. We measured the percentage of disrupted CCR5 alleles in the blood of mice at sequential time points after HIV-1 challenge, using both the Cel 1 assay and a specific PCR amplification that detects a common 5-bp duplication at the ZFN target site that typically accounts for 10–30% of total modifications<sup>19</sup>. Both assays revealed a rapid increase in the frequency of ZFN-disrupted alleles, reaching the upper limit of the Cel 1 assay by 4 weeks after infection (Fig. 4a).

We also examined levels of CCR5 disruption in multiple tissues from ZFN-treated animals, either uninfected or 12 weeks after HIV-1<sub>BAL</sub> challenge, and observed a sharp increase in CCR5 disruption after HIV-1 infection (Fig. 4b). FACS analysis of the spleen and intestine revealed that, in contrast to uninfected animals, in which ~25% of CD4<sup>+</sup> cells were also CCR5<sup>+</sup>, very little or no CCR5 expression was detected in the CD4<sup>+</sup> T cells that persisted in the ZFN-treated animals (Fig. 4c,d). Together, these data suggest that the protection of CD4<sup>+</sup> lymphocytes in ZFN-treated mice was a consequence of selection for CCR5<sup>-</sup>, HIV-1-resistant cells derived from ZFN-edited cells.

### Heterogeneity of CCR5 modifications suggests polyclonal origins

ZFN-induced double-stranded breaks repaired by nonhomologous end-joining result in highly heterogeneous changes at the targeted locus<sup>19</sup>. We used this property to investigate whether the CCR5<sup>-</sup> cells that developed in mice that received ZFN-treated CD34<sup>+</sup> HSPCs were polyclonal in origin. Sequencing of 60 individual CCR5 alleles amplified from the large intestine of an HIV-1-infected mouse into which ZFN-treated CD34<sup>+</sup> HSPCs were previously transplanted revealed that 59 alleles harbored mutations at the ZFN target site (Fig. 5). As previously

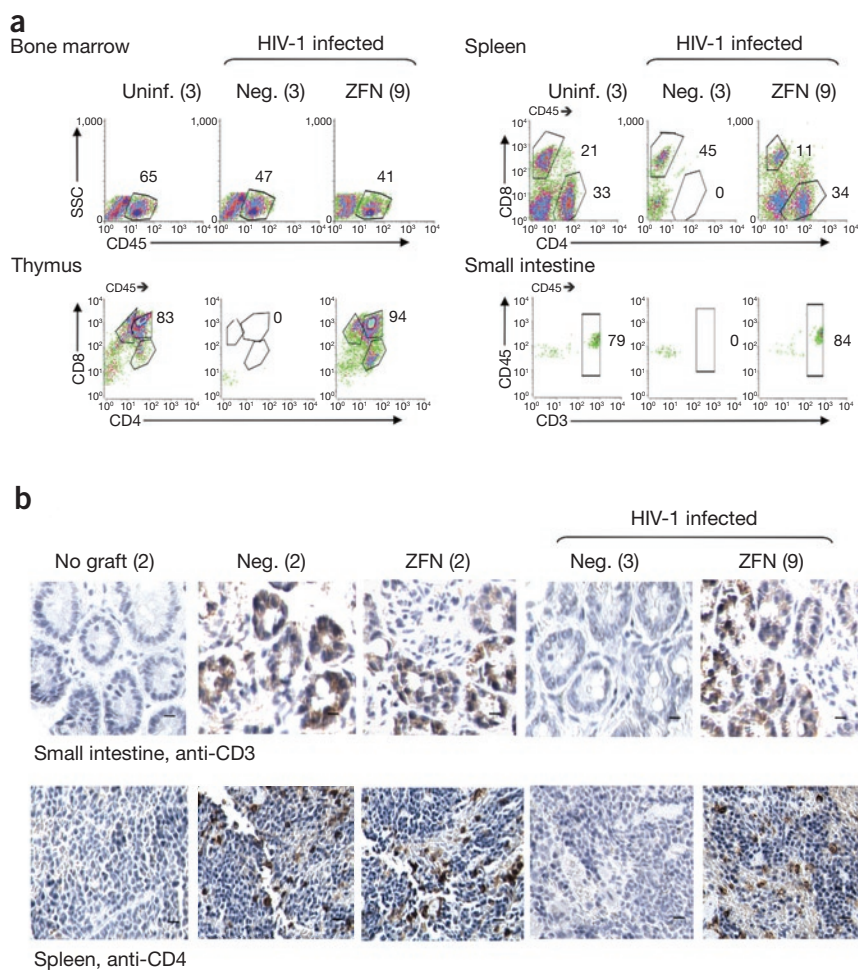


**Figure 3** Effects of HIV-1 infection on human cells in HSPC-engrafted NSG mice. **(a)** FACS analysis of human cells in tissues of representative NSG mice from three cohorts: uninfected mice previously engrafted with either untreated or ZFN-treated CD34<sup>+</sup> HSPCs (Uninf.), and HIV-1 infected animals previously engrafted with either untreated (Neg.) or ZFN-treated (ZFN) CD34<sup>+</sup> HSPCs. Mice were necropsied at 12 weeks post-infection or at the equivalent time point for uninfected animals. The total number of animals analyzed in each cohort is indicated. FACS analysis was performed as described in Figure 1. Small intestine sample is lamina propria, and similar results were obtained when samples from the large intestine were analyzed. Percentage of cells in indicated compartments is shown. **(b)** Immunohistochemical analysis of human CD3 expression in small intestine, and CD4 expression in spleen of representative NSG mice, into which untreated (Neg.) or ZFN-treated (ZFN) CD34<sup>+</sup> HSPCs were transplanted, with and without HIV-1 infection. Animals were necropsied at 12 weeks after infection or at the same time point for uninfected animals. Control animals receiving no human CD34<sup>+</sup> HSPCs (no graft) were also analyzed. The number of animals analyzed in each cohort is shown. Scale bars, 50 μm.

reported for this ZFN pair<sup>19</sup>, a high proportion (13 out of 59) of the mutated loci contained a characteristic 5-bp duplication, with the remaining 46 clones bearing 36 unique sequences. In contrast, all alleles sequenced from a mouse receiving untreated CD34<sup>+</sup> HSPCs contained the wild-type sequence (data not shown). The high degree of sequence diversity observed strongly suggests that multiple stem or progenitor cells were modified by the ZFNs. These findings also predict that the overwhelming majority of cells selected by HIV-1<sub>BAL</sub> infection would be *CCR5*<sup>-/-</sup>, which is in agreement with the data from flow cytometry analysis (Fig. 4c).

#### Presence of ZFN-modified cells controls HIV-1 replication *in vivo*

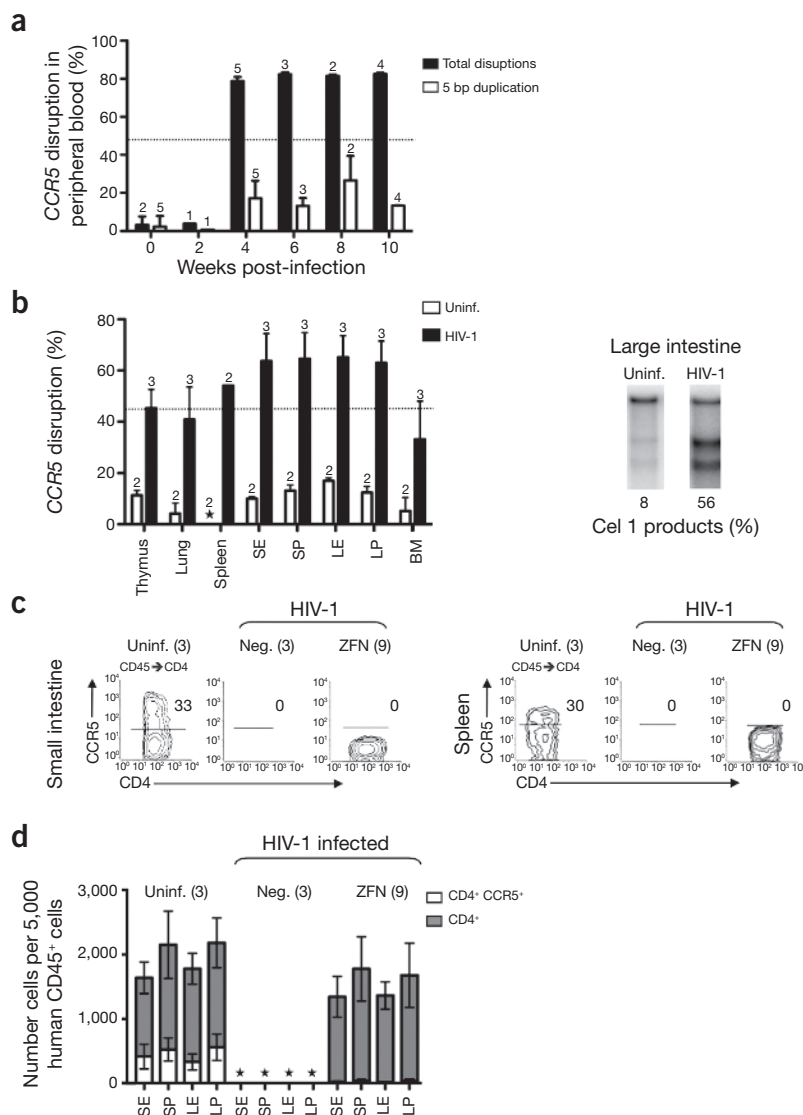
Quantitative PCR analysis of HIV-1 RNA levels in the peripheral blood of animals revealed that peak viremia occurred at 6 weeks after infection for animals that received transplants of either untreated or ZFN-treated CD34<sup>+</sup> HSPCs (Fig. 6a), although the levels were significantly lower ( $P = 0.03$ ) in the ZFN cohort. By 8 weeks after infection, viral loads in both cohorts were dropping but there continued to be a statistically significant difference between the two groups ( $P = 0.001$ ). Measurements of p24 levels in the blood by enzyme-linked immunosorbent assay (ELISA) corroborated these findings, with a

significant difference ( $P = 0.02$ ) in antigenemia between the two groups observed by the 6-week time point (data not shown).

These differences between the two cohorts are more striking when the levels of human CD4<sup>+</sup> T cells are also considered (Fig. 6a), as the loss of CD4<sup>+</sup> T cells in the untreated mice probably contributed to the lowering of overall viral levels seen as the infection progressed. The continued presence of virus in the blood, despite acute loss of CD4<sup>+</sup> cells, also occurs during progression to AIDS, where high viral load measurements in serum are typically observed when T-cell death is rapidly occurring<sup>41</sup>. In contrast, CD4<sup>+</sup> T-cell levels in the ZFN-treated mice rebounded after the 2-week nadir and recovered to normal levels by 4 weeks after infection. In contrast to these findings with HIV-1<sub>BAL</sub>, ZFN-treated mice challenged with a CXCR4-tropic HIV-1 strain did not control viral levels or preserve CD4<sup>+</sup> T cells, confirming that the mechanism is *CCR5* specific (Supplementary Fig. 4).

We also measured HIV-1 levels in intestinal samples. In tissues harvested at 8 and 9 weeks after infection, viral levels in the ZFN-treated mice were 4 orders of magnitude lower than in the untreated controls. By the 10- and 12-week time points, HIV-1 RNA was undetectable in the ZFN-treated mice (Fig. 6c). This drop in viral load occurred despite the maintenance of normal numbers of human

**Figure 4** HIV-1 infection selects for disrupted *CCR5* alleles. **(a)** Mean  $\pm$  s.d. levels of *CCR5* disruption (Cel 1 assay, black bars) in sequential peripheral blood samples taken from mice into which ZFN-treated CD34<sup>+</sup> HSPCs were transplanted and which were subsequently infected with HIV-1. Upper limit of linearity of Cel 1 assay is 44% (ref. 19) and is indicated by the dotted line; upper limit of sensitivity of assay is 70–80%. White bars show the frequency of a common 5-bp duplication at the ZFN target site that typically comprises 10–30% of total *CCR5* mutations<sup>19</sup>. Numbers of mice analyzed at each time point, and in each assay, are shown above the appropriate bar. **(b)** Mean  $\pm$  s.d. levels of *CCR5* disruption (Cel 1 assay) in indicated tissues from mice into which ZFN-treated CD34<sup>+</sup> HSPCs were transplanted; mice were necropsied at 12 weeks after infection (black bars) or at an equivalent time point for uninfected ZFN-treated animals (white bars). Numbers analyzed in each group are shown above the appropriate bar. One representative Cel 1 analysis from the large intestine (lamina propria) of uninfected and infected mice is shown. Animals receiving untreated cells gave no Cel 1 digestion products at any time point analyzed (data not shown). Asterisk indicates levels too low to quantify. **(c)** Contour FACS analyses of human CD4<sup>+</sup> cells in the small intestine (lamina propria) and spleen of one representative animal from each indicated cohort are shown. Cells were gated on FSC/SSC to remove debris and gated on human CD45 and CD4. Numbers indicate the percentage of cells that are *CCR5*<sup>+</sup>. **(d)** Mean  $\pm$  s.d. numbers of human CD4<sup>+</sup> cells (gray bars) and CD4<sup>+</sup>*CCR5*<sup>+</sup> cells (white bars) per 5,000 human CD45<sup>+</sup> cells analyzed from different sections of the intestine and from the indicated cohorts. Asterisk indicates levels too low to quantify. Number of animals analyzed in each cohort is indicated. Abbr. S, small intestine; L, large intestine; E, intraepithelial lymphocytes; P, lamina propria lymphocytes; BM, bone marrow.



## Wild-type (1)

gttttgtgggcaacatgctggtcacctcatcctgataaaactgcaaaaggctgaagagcatgactgaca wt

## Deletions (43)

gttttgtgggcaacatgctggtcacctcatcctgataaaactgcaaaaggctgaagagcatgactgaca -1  
 gttttgtgggcaacatgctggtcacctcatcctgat--actgcaaaaggctgaagagcatgactgaca -2  
 gttttgtgggcaacatgctggtcacctcatcctg--aaactgcaaaaggctgaagagcatgactgaca -2 2X  
 gttttgtgggcaacatgctggtcaccc---tctgataaaactgcaaaaggctgaagagcatgactgaca -3  
 gttttgtgggcaacatgctggtcacctcatc---taaactgcaaaaggctgaagagcatgactgaca -4  
 gttttgtgggcaacatgctggtcacctcatc-----aaactgcaaaaggctgaagagcatgactgaca -5 3X  
 gttttgtgggcaacatgctggAcacctcatcctgat-----caaaaggctgaagagcatgactgaca -6  
 gttttgtgggcaacatgctggtcacctcatc-----aaTtgcaaaaggctgaagagcatgactgaca -6  
 gttttgtgggcaacatgctggtcacctcatcctgat-----aaaaggctgaagagcatgactgaca -7  
 gttttgtgggcaacatgctggtcac-----ctgataaaactgcaaaaggctgaagagcatgactgaca -7  
 gttttgtgggcaacatgctggtcacctcatc-----ctgcaaaaggctgaagagcatgactgaca -8  
 gttttgtgggcaacatgctggtcacctcatcctgat-----aaaggctgaagagcatgactgaca -8  
 gttttgtgggcaacatgctggtcacctc-----aaactgcaaaaggctgaagagcatgactgaca -8  
 gttttgtgggcaacatgctggtcaccc-----ataaactgcaaaaggctAaagagcatgactgaca -8  
 gttttgtgggcaacatgctggtcacctcat-----ctgcaaaaggctgaagagcatgactgaca -9  
 gttttgtgggcaacatgctggtcacctcatcctgat-----agctgaagagcatgactgaca -10  
 gttttgtgggcaacatgctggtcacctcatc-----caaaaggctgaagagcatgactgaca -10  
 gttttgtgggcaacatgctggtcacctca-----tgcaaaaggctgaagagcatgactgaca -11 2X  
 gttttgtgggcaacatgctggtcacctcatc-----aaaaggctgaaAagGatgactgaca -12  
 gttttgtgggcaacatgctg-----ctgGtaaaactgcaaaaggctgaagagcatgactgaca -12  
 gttttgtgggcaacatgctggtcacct-----gcaaaaggctgaagagcatgactgaca -14 5X  
 gttttgtgggcaacatgctggtcac-----ctgcaaaaggctgaagagcatgactgaca -15  
 gttttgtgggcaacatgctggtcacct-----caaaaggctgaagagcatgactgaca -15 2X  
 gttttgtgggcaacatgctggtcacctcatcctgataa-----gagcatgactgaca -16  
 gttttgtgggcaacatgctggtcacctcatcctgat-----Cgagcatgactgaca -17  
 gttttgtgggcaacatgctggtcacctcatcctga-----gagcatgactgaca -19  
 gttttgtgggcaacatgctggtcacctcatc-----tgaagagcatgactgaca -19  
 gttttgtgggcaacatgctggtcacctcatcctgat-----gcatgactgaca -20  
 gttttgtgggcaacatgctggtcacctcatc-----agagcatgactgaca -22  
 gttttgtgggcaacatgc-----aaaaggctgaagagcatgactgaca -26  
 gttttgtgggcaa-----caaaaggctgaagagcatgactgaca -30  
 gttttgtgggcaacatgctggtcacctcatcctg-----ca -32  
 gttttgtgggcaacatgctggtcacctcatcctg-----ca -45

## Insertions (16)

gttttgtgggcaacatgctggtcacctcatcctCTgataaaactgcaaaaggctgaagagcatgactga +2  
 gttttgtgggcaacatgctggtcacctcatcctcatcctgataTAaactgcaaaaggctgaagagcatgactga +2  
 gttttgtgggcaacatgctggtcacctcatcctcatcctgatCTGATAaactgcaaaaggctgaagagcatgac +5 13X

T lymphocytes in the intestines and other tissues (Fig. 3). These observations are consistent with a strong selective pressure for HIV-resistant *CCR5*<sup>-/-</sup> cells to replace *CCR5*-expressing cells, leading to control of viral replication.

## DISCUSSION

Despite major advances in anti-retroviral therapy, HIV-1 infection remains an epidemic cause of morbidity and mortality. Effective anti-retroviral therapy often involves costly, multi-drug regimens that are not well tolerated by a significant percentage of patients<sup>42</sup>, and even successful adherence to the therapy does not eradicate the virus, and a rapid rebound in HIV-1 levels can occur if therapy is discontinued<sup>43</sup>. An alternative approach to controlling HIV-1 replication is engineering of the body's immune cells to be resistant to infection<sup>44</sup>. In this regard, the *CCR5* co-receptor is an attractive target because of the HIV-resistant phenotype of homozygous *CCR5*Δ32 individuals<sup>3</sup>. In the present study, we identified conditions that allow efficient disruption of *CCR5* in human CD34<sup>+</sup> HSPCs and demonstrated that such modified cells generate *CCR5*<sup>-/-</sup>, HIV-resistant progeny in a mouse model of human hematopoiesis and HIV-1 infection, leading to control of HIV-1 replication. These findings suggest that transplantation of autologous HSPCs modified by *CCR5*-specific ZFNs may provide a permanent supply of HIV-resistant progeny that could replace cells killed by HIV-1, reconstitute the immune system and control viral replication long term in the absence of anti-retroviral therapy.

The high levels of *CCR5* disruption that we achieved were possible because of an efficient gene editing technology based on ZFNs. ZFNs can be designed to bind to a specific genomic DNA sequence

**Figure 5** ZFN activity produces heterogeneous mutations in *CCR5*. Sequence analysis was performed on 60 cloned human *CCR5* alleles, PCR amplified from intraepithelial cells from the large intestine of an HIV-infected mouse into which ZFN-treated CD34<sup>+</sup> HSPCs were previously transplanted, and at 12 weeks post-infection. The number of nucleotides deleted or inserted at the ZFN target site (underlined) in each clone is indicated on the right of each sequence, together with the number of times the sequence was found. Dashes (-) indicate deleted bases compared to the wild-type sequence; uppercase letters are point mutations; underlined uppercase letters are inserted bases. Some specific mutations of *CCR5* occurred more frequently, in particular a 5-bp duplication at the ZFN target site that was identified 13 times (bottom sequence). No mutations in *CCR5* were observed in a similar analysis performed on control samples from a mouse receiving unmodified CD34<sup>+</sup> HSPCs (data not shown).

and effect permanent knockout of the targeted gene<sup>19,45–47</sup>. Only transient expression of the ZFNs is required during a brief period of *ex vivo* culture, and the genetic mutation is present for the life of the cell and its progeny. Thus, a major shortcoming of other gene therapy technologies—the need for continued expression of a foreign transgene—is avoided. Moreover, unlike approaches based on small molecules, antibodies or RNA interference<sup>44</sup>, ZFN-mediated gene disruption can completely eliminate *CCR5* from the surface of

cells through bi-allelic modification. By using an optimized nucleofection procedure, we were able to overcome the technical challenges to ZFN-induced genome editing in CD34<sup>+</sup> cells previously reported<sup>21</sup> and achieve, on average, disruption at 17% of the loci, which we estimate will produce 5–7% bi-allelically modified cells.

The safety and efficacy of T lymphocytes modified with *CCR5*-targeted ZFNs are currently being evaluated in a phase I clinical trial. In a preclinical study, investigation of the specificity of the same *CCR5*-targeted ZFNs as used in this study revealed off-target cleavage events in T cells at significant levels only at the homologous *CCR2* locus<sup>19</sup>. Studies in mice have not detected any deleterious phenotype associated with loss of *CCR2* (ref. 48), and human genetic studies have even suggested a beneficial phenotype from the loss of this gene in HIV-infected individuals<sup>49</sup>. Although not analyzed here, modification of CD34<sup>+</sup> HSPCs with these same *CCR5* ZFN reagents is likely to result in similar, low levels of off-target cleavage events. Any safety concerns associated with nonspecific cleavage must be evaluated in larger, future studies.

Although T lymphocytes are the primary target of HIV-1 infection, ZFN modification of HSPCs may allow longer-term production of *CCR5*<sup>-/-</sup> cells in patients. The scientific rationale for *CCR5* modification of HSPCs is supported by the recent finding that an HIV<sup>+</sup> leukemia patient receiving a transplant from a *CCR5*<sup>-/-</sup> donor was effectively cured of his infection, despite discontinuing antiretroviral therapy<sup>9</sup>. As shown by our data, ZFN-modified HSPCs retained full functionality and gave rise to *CCR5*<sup>-</sup> cells in lineages relevant to HIV-1 pathogenesis. ZFNs delivered to purified CD34<sup>+</sup> cell populations by nucleofection were capable of modifying true SCID-repopulating stem cells, and the high levels of *CCR5* editing were maintained after secondary transplantation.



The experimental mouse model of HIV-1 infection used in these studies revealed a strong selection for  $CCR5^{-}$  progeny during acute infection with a  $CCR5$ -tropic strain of HIV-1. This suggests that  $CCR5^{-/-}$  stem cells, even if the minority, produced sufficient numbers of  $CCR5^{-/-}$  progeny to support immune reconstitution and inhibit HIV-1 replication. Such selection is consistent with clinical observations from genetic diseases such as adenosine deaminase deficiency (ADA)-SCID, X-linked SCID and Wiskott-Aldrich syndrome, in which normal hematopoietic cells have a selective advantage, so that spontaneous monoclonal reversions can lead to selective outgrowth of such cells and amelioration of symptoms<sup>50–53</sup>.

The observation of almost complete replacement of human T cells in the intestines of the infected mice with  $CCR5^{-}$  cells is consistent with this tissue harboring the majority of the body's  $CD4^{+}CCR5^{+}$  effector memory cells. A characteristic feature of HIV-1 replication in mucosal tissues is an ongoing cycle of T-cell death and the recruitment of replacement T cells, which, in an activated state, are highly permissive for HIV-1 infection<sup>37</sup>. This is especially true in the gut mucosa, a key battleground in HIV-1 infection<sup>54–56</sup>. We also observed a strong selection for  $CCR5^{-}$  cells in the thymus, suggesting that  $CCR5^{-}$  cells would be selected at both a precursor stage in the thymus and at an effector stage in the mucosa. Ultimately, the presence of HIV-resistant  $CCR5^{-}$  cells in mucosal tissues should both protect individual cells from infection and help to break the cycle of immune hyperactivation that may underlie much of the pathology of AIDS<sup>57</sup>.

Although antiretroviral therapy is highly effective in many patients, the associated costs and potential for side effects can be considerable when extrapolated over a lifetime. In contrast, our approach may provide a one-shot treatment that would be most suited to the setting of autologous HSPC transplantation. Procedures for isolating and processing HSPCs for autologous or allogeneic transplantation are well established. The use of a patient's own stem cells may remove the requirement for full ablation of the marrow hematopoietic compartment and the immune suppression that is necessary in allogeneic transplantation. Indeed, the toxicity of such regimens is one reason that allogeneic stem cell transplantation from  $CCR5\Delta32$  donors is not a realistic treatment option for HIV<sup>+</sup> patients in the absence of other conditions that necessitate the transplant.

Of note, certain HIV-infected individuals, such as AIDS lymphoma patients, already undergo full ablation and autologous HSPC rescue as part of their therapy<sup>58</sup> and may be suitable candidates for HSPC-based gene therapies<sup>44</sup>. In addition, the experience of autologous HSPC transplantation in gene therapy treatments for ADA-SCID<sup>59,60</sup>, chronic granulomatous disease<sup>61</sup> and X-linked adrenoleukodystrophy<sup>62</sup> is that nonmyeloablative conditioning can facilitate engraftment of gene-modified autologous HSPCs with minimal associated toxicity. It is possible that the use of nonmyeloablative regimens, together with the selective advantage conferred on  $CCR5^{-/-}$  progeny, could prove an effective combination for HIV<sup>+</sup> patients receiving ZFN-treated autologous HSPCs.

Targeting  $CCR5$  is not expected to provide protection against viruses that use alternate co-receptors such as CXCR4. Although only a handful of cases of HIV-1 infection of  $CCR5\Delta32$  homozygotes have been reported<sup>63,64</sup>, CXCR4-tropic viruses have been associated with accelerated disease progression<sup>65</sup>, so that selection for such strains could be an undesirable consequence of targeting  $CCR5$ . However, this outcome is not generally observed in patients treated with  $CCR5$  inhibitors unless CXCR4-tropic viruses were present before therapy, and resistance to these drugs occurs by viral adaptation to the drug-bound form of  $CCR5$  (refs. 66,67). Notably, although the patient who received the  $CCR5\Delta32$  transplant harbored CXCR4-tropic virus before the procedure, his HIV-1 infection was still controlled long term<sup>9,10</sup>. Similar to the recommendations for  $CCR5$  inhibitors, it may be prudent to restrict  $CCR5$  ZFN treatment of HSPCs to individuals with no detectable CXCR4-tropic virus.

In contrast to the acute HIV-1 infection modeled in this study, HIV-1 patients usually present in a chronic phase of the disease, and their viral levels can be effectively controlled by antiretroviral therapy. The requirement for the selective pressure of active HIV-1 replication in the success of this, or other, anti-HIV gene therapies is at present unknown. It has been suggested that low-level viral replication continues in certain sanctuary sites, even in well-controlled patients on antiretroviral therapy<sup>43,68</sup>, which could provide a low level of selection, although drug intensification trials have not provided evidence of ongoing replication<sup>69</sup>. It is also possible that the high levels of  $CCR5$  disruption we achieved without selection, if extrapolated to HIV<sup>+</sup> patients, could be sufficient to provide a therapeutic effect even in the absence of a strong selective pressure. Alternatively, ZFN knockout of  $CCR5$  in HSPCs could be viewed as a backup strategy in the event that antiretroviral therapy fails or is withdrawn. It may also be possible to incorporate antiretroviral therapy interruptions into an overall therapeutic strategy, as recently described for HIV-infected individuals receiving autologous HSPCs engineered with anti-HIV ribozymes, where gene-marked progeny were found at higher levels after treatment interruptions<sup>70</sup>.

In summary, our data demonstrate that transient ZFN treatment of human  $CD34^{+}$  HSPCs can efficiently disrupt  $CCR5$  while yielding cells that remain competent to engraft and support hematopoiesis. In the presence of  $CCR5$ -tropic HIV-1,  $CCR5^{-/-}$  progeny rapidly replaced cells depleted by the virus, leading to a polyclonal population that ultimately

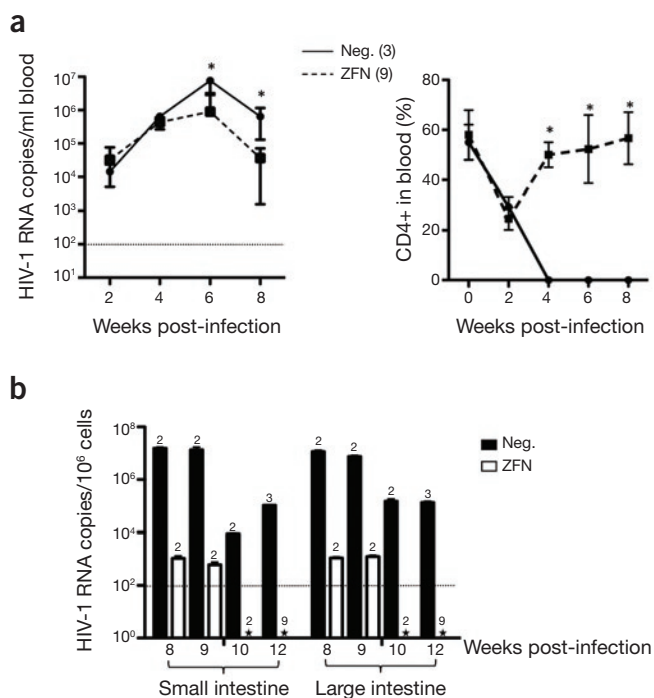


**Figure 6** Control of HIV-1 replication in mice receiving ZFN-treated  $CD34^{+}$  HSPCs. (a) Mean  $\pm$  s.d. levels of HIV-1 RNA (left) and percent  $CD4^{+}$  human T cells (right) in peripheral blood of mice into which untreated (Neg.) or ZFN-treated  $CD34^{+}$  HSPCs were transplanted, at indicated times post-infection. Dashed line is limit of detection of assay. Asterisk indicates a statistically significant difference between two groups ( $P < 0.05$ ). (b) Mean  $\pm$  s.d. HIV-1 RNA levels in small and large intestine lamina propria from Neg. or ZFN mice, from animals necropsied between 8 and 12 weeks post-infection. Numbers of mice analyzed at each time point are shown above the appropriate bar. Dashed line indicates limits of detection of assay. Asterisk indicates undetectable levels.

preserved human immune cells in multiple tissues. Our findings indicate that the modification of only a minority of human CD34<sup>+</sup> HSPCs may provide the same strong anti-viral benefit as was conferred by a complete CCR5Δ32 stem cell transplantation in a patient<sup>9</sup>. And they further suggest that a partially modified autologous transplant, administered under only mildly ablative transplantation regimens may also be effective, opening up the treatment to many more HIV-infected individuals. Finally, the identification of conditions that allow the efficient use of ZFNs in human CD34<sup>+</sup> HSPCs suggests the use of this technology in other diseases for which HSPC modification may be curative.

## METHODS

Methods and any associated references are available in the online version of the paper at <http://www.nature.com/naturebiotechnology/>.

Note: Supplementary information is available on the Nature Biotechnology website.

## ACKNOWLEDGMENTS

We would like to thank A. Cuddihy, S. Ge, R. Hollis and N. Smiley for expert technical assistance; C. Lutzko, V. Garcia, R. Akkina, B. Torbett and M. McCune for advice regarding humanized mice; and M. McCune for communicating unpublished data. This work was supported by funding from the California HIV/AIDS Research Project (P.M.C.), The Saban Research Institute (V.T.), and the National Heart, Lung, and Blood Institute P01 HL73104 (G.M.C., D.B.K. and P.M.C.).

## AUTHOR CONTRIBUTIONS

N.H. performed most of the experiments; J.W., K.K., G.F. and X.W. developed assays and analyzed samples; V.T. contributed to discussions; N.H., G.M.C., D.B.K., P.D.G., M.C.H. and P.M.C. designed the experiments and analyzed data; N.H. and P.M.C. wrote the manuscript.

## COMPETING FINANCIAL INTERESTS

The authors declare competing financial interests: details accompany the full-text HTML version of the paper at <http://www.nature.com/naturebiotechnology/>.

Published online at <http://www.nature.com/naturebiotechnology/>.

Reprints and permissions information is available online at <http://npg.nature.com/reprintsandpermissions/>.

- Wu, L. *et al.* CD4-induced interaction of primary HIV-1 gp120 glycoproteins with the chemokine receptor CCR-5. *Nature* **384**, 179–183 (1996).
- deRoda Husman, A.M., Blaak, H., Brouwer, M. & Schuitemaker, H. CC chemokine receptor 5 cell-surface expression in relation to CC chemokine receptor 5 genotype and the clinical course of HIV-1 infection. *J. Immunol.* **163**, 84597–84603 (1999).
- Samson, M. *et al.* Resistance to HIV-1 infection in Caucasian individuals bearing mutant alleles of the CCR-5 chemokine receptor gene. *Nature* **382**, 722–725 (1996).
- Novembre, J. *et al.* The geographic spread of the CCR5 Delta32 HIV-resistance allele. *PLoS Biol.* **3**, e339 (2005).
- Glass, W.G. *et al.* CCR5 deficiency increases risk of symptomatic West Nile virus infection. *J. Exp. Med.* **203**, 35–40 (2006).
- Kantarci, O.H. *et al.* CCR5Δ32 polymorphism effects on CCR5 expression, patterns of immunopathology and disease course in multiple sclerosis. *J. Neuroimmunol.* **169**, 137–143 (2005).
- Rosol, M. *et al.* Negative association of the chemokine receptor CCR5 d32 polymorphism with systemic inflammatory response, extra-articular symptoms and joint erosion in rheumatoid arthritis. *Arthritis Res. Ther.* **11**, R91–98 (2009).
- Dau, B. & Holodiny, M. Novel targets for antiretroviral therapy: clinical progress to date. *Drugs* **69**, 31–50 (2009).
- Hutter, G. *et al.* Long-term control of HIV by CCR5 Delta32/Delta32 stem-cell transplantation. *N. Engl. J. Med.* **360**, 692–698 (2009).
- Hutter, G., Schneider, T. & Thiel, E. Transplantation of selected or transgenic blood stem cells—a future treatment for HIV/AIDS? *J. Int. AIDS Soc.* **12**, 10–14 (2009).
- Anderson, J. *et al.* Safety and efficacy of a lentiviral vector containing three anti-HIV genes—CCR5 ribozyme, tat-rev siRNA, and TAR decoy—in SCID-hu mouse-derived T cells. *Mol. Ther.* **15**, 1182–1188 (2007).
- Bai, J. *et al.* Characterization of anti-CCR5 ribozyme-transduced CD34<sup>+</sup> hematopoietic progenitor cells in vitro and in a SCID-hu mouse model in vivo. *Mol. Ther.* **1**, 244–254 (2000).
- Kumar, P. *et al.* T cell-specific siRNA delivery suppresses HIV-1 infection in humanized mice. *Cell* **134**, 577–586 (2008).
- Swan, C.H. *et al.* T-cell protection and enrichment through lentiviral CCR5 intrabody gene delivery. *Gene Ther.* **13**, 1480–1492 (2006).
- Swan, C.H. & Torbett, B.E. Can gene delivery close the door to HIV-1 entry after escape? *J. Med. Primatol.* **35**, 236–247 (2006).
- Urnov, F.D. *et al.* Highly efficient endogenous human gene correction using designed zinc-finger nucleases. *Nature* **435**, 646–651 (2005).
- Jasin, M. *et al.* Genetic manipulation of genomes with rare-cutting endonucleases. *Trends Genet.* **12**, 224–228 (1996).
- Sonoda, E. *et al.* Differential usage of non-homologous end-joining and homologous recombination in double strand break repair. *DNA Repair (Amst.)* **5**, 1021–1029 (2006).
- Perez, E.E. *et al.* Establishment of HIV-1 resistance in CD4<sup>+</sup> T cells by genome editing using zinc-finger nucleases. *Nat. Biotechnol.* **26**, 808–816 (2008).
- Ishikawa, F. *et al.* Development of functional human blood and immune systems in NOD/SCID/IL2 receptor (gamma) chain(null) mice. *Blood* **106**, 1565–1573 (2005).
- Lombardo, A. *et al.* Gene editing in human stem cells using zinc finger nucleases and integrase-defective lentiviral vector delivery. *Nat. Biotechnol.* **25**, 1298–1306 (2007).
- Hollis, R.P. *et al.* Stable gene transfer to human CD34(+) hematopoietic cells using the Sleeping Beauty transposon. *Exp. Hematol.* **34**, 1333–1343 (2006).
- Sumiyoshi, T. *et al.* Stable transgene expression in primitive human CD34<sup>+</sup> hematopoietic stem/progenitor cells, using the Sleeping Beauty transposon system. *Hum. Gene Ther.* **20**, 1607–1626 (2009).
- Mátés, L. *et al.* Molecular evolution of a novel hyperactive Sleeping Beauty transposase enables robust stable gene transfer in vertebrates. *Nat. Genet.* **41**, 753–761 (2009).
- Xue, X. *et al.* Stable gene transfer and expression in cord blood-derived CD34<sup>+</sup> hematopoietic stem and progenitor cells by a hyperactive Sleeping Beauty transposon system. *Blood* **114**, 1319–1330 (2009).
- Basu, S. & Broxmeyer, H.E. CCR5 ligands modulate CXCL12-induced chemotaxis, adhesion, and Akt phosphorylation of human cord blood CD34<sup>+</sup> cells. *J. Immunol.* **183**, 7478–7488 (2009).
- Watanabe, S. *et al.* Hematopoietic stem cell-engrafted NOD/SCID/IL2Rgamma null mice develop human lymphoid systems and induce long-lasting HIV-1 infection with specific humoral immune responses. *Blood* **109**, 212–218 (2007).
- Brenchley, J.M. *et al.* CD4<sup>+</sup> T cell depletion during all stages of HIV disease occurs predominantly in the gastrointestinal tract. *J. Exp. Med.* **200**, 749–759 (2004).
- Brenchley, J.M. *et al.* HIV disease: fallout from a mucosal catastrophe? *Nat. Immunol.* **7**, 235–239 (2006).
- Guadalupe, M. *et al.* Severe CD4<sup>+</sup> T-cell depletion in gut lymphoid tissue during primary human immunodeficiency virus type 1 infection and substantial delay in restoration following highly active antiretroviral therapy. *J. Virol.* **77**, 11708–11717 (2003).
- Talal, A.H. *et al.* Effect of HIV-1 infection on lymphocyte proliferation in gut-associated lymphoid tissue. *J. Acquir. Immune Defic. Syndr.* **26**, 208–217 (2001).
- Li, Q. *et al.* Peak SIV replication in resting memory CD4<sup>+</sup> T cells depletes gut lamina propria CD4<sup>+</sup> T cells. *Nature* **434**, 1148–1152 (2005).
- Mattapallil, J.J. *et al.* Massive infection and loss of memory CD4<sup>+</sup> T cells in multiple tissues during acute SIV infection. *Nature* **434**, 1093–1097 (2005).
- Veazey, R.S. *et al.* Gastrointestinal tract as a major site of CD4<sup>+</sup> T cell depletion and viral replication in SIV infection. *Science* **280**, 427–431 (1998).
- Berges, B.K. *et al.* HIV-1 infection and CD4 T cell depletion in the humanized Rag2-/-gamma c-/- (RAG-hu) mouse model. *Retirovirology* **3**, 76–90 (2006).
- Appay, V. & Sauce, D. Immune activation and inflammation in HIV-1 infection: causes and consequences. *J. Pathol.* **214**, 231–241 (2008).
- Stoddart, C.A. *et al.* IFN-alpha-induced upregulation of CCR5 leads to expanded HIV tropism in vivo. *PLoS Pathog.* **6**, e1000766 (2010).
- Choudhary, S.K. *et al.* R5 human immunodeficiency virus type 1 infection of fetal thymic organ culture induces cytokine and CCR5 expression. *J. Virol.* **79**, 458–471 (2005).
- Kahn, J.O. & Walker, B.D. Acute human immunodeficiency virus type 1 infection. *N. Engl. J. Med.* **339**, 33–39 (1998).
- Margolick, J.B. *et al.* Impact of inversion of the CD4/CD8 ratio on the natural history of HIV-1 infection. *J. Acquir. Immune Defic. Syndr.* **42**, 620–626 (2007).
- Henrard, D.R. *et al.* Natural History of HIV-1 cell-free viremia. *J. Am. Med. Assoc.* **274**, 554–558 (1995).
- Chen, R.Y. *et al.* Distribution of health care expenditures for HIV-infected patients. *Clin. Infect. Dis.* **42**, 1003–1010 (2006).
- Richman, D.D. *et al.* The challenge of finding a cure for HIV infection. *Science* **323**, 1304–1307 (2009).
- Rossi, J.J., June, C.H. & Kohn, D.B. Genetic therapies against HIV. *Nat. Biotechnol.* **25**, 1444–1454 (2007).
- Bibikova, M. *et al.* Targeted chromosomal cleavage and mutagenesis in *Drosophila* using zinc-finger nucleases. *Genetics* **161**, 1169–1175 (2002).
- Doyon, Y. *et al.* Heritable targeted gene disruption in zebrafish using designed zinc-finger nucleases. *Nat. Biotechnol.* **26**, 702–708 (2008).
- Santiago, Y. *et al.* Targeted gene knockout in mammalian cells by using engineered zinc-finger nucleases. *Proc. Natl. Acad. Sci. USA* **105**, 5809–5814 (2008).
- Peters, W., Dupuis, M. & Charo, I.F. A mechanism for the impaired IFN-gamma production in C-C chemokine receptor 2 (CCR2) knockout mice: Role of CCR2 in linking the innate and adaptive immune responses. *J. Immunol.* **165**, 7072–7077 (2000).
- Smith, M.W. *et al.* CCR2 chemokine receptor and AIDS progression. *Nat. Med.* **3**, 1052–1053 (1997).
- Davis, B.R. & Candotti, F. Revertant somatic mosaicism in the Wiskott-Aldrich syndrome. *Immunol. Res.* **44**, 127–131 (2009).
- Hirschhorn, R. *et al.* Spontaneous in vivo reversion to normal of an inherited mutation in a patient with adenosine deaminase deficiency. *Nat. Genet.* **3**, 290–295 (1996).



52. Hirschhorn, R. *et al.* In vivo reversion to normal of inherited mutations in humans. *J. Med. Genet.* **40**, 721–728 (2003).
53. Stephan, V. *et al.* Atypical X-linked severe combined immunodeficiency due to possible spontaneous reversion of the genetic defect in T cells. *N. Engl. J. Med.* **335**, 1563–1567 (1996).
54. Chun, T.W. *et al.* Persistence of HIV in gut-associated lymphoid tissue despite long-term antiretroviral therapy. *J. Infect. Dis.* **197**, 714–720 (2008).
55. Lackner, A.A. *et al.* The gastrointestinal tract and AIDS pathogenesis. *Gastroenterology* **136**, 1965–1978 (2009).
56. Picker, L.J. Immunopathogenesis of acute AIDS virus infection. *Curr. Opin. Immunol.* **18**, 399–405 (2006).
57. Veazey, R.S., Marx, P.A. & Lackner, A.A. The mucosal immune system: primary target for HIV infection and AIDS. *Trends Immunol.* **22**, 626–633 (2001).
58. Krishnan, A. *et al.* Autologous stem cell transplantation for HIV associated lymphoma. *Blood* **98**, 3857–3859 (2001).
59. Aiuti, A. *et al.* Correction of ADA-SCID by stem cell gene therapy combined with nonmyeloablative conditioning. *Science* **296**, 2410–2413 (2002).
60. Aiuti, A. *et al.* Gene therapy for immunodeficiency due to adenosine deaminase deficiency. *N. Engl. J. Med.* **360**, 447–458 (2009).
61. Ott, M.G. *et al.* Correction of X-linked chronic granulomatous disease by gene therapy, augmented by insertional activation of MDS1–EV11, PRDM16 or SETBP1. *Nat. Med.* **12**, 401–409 (2006).
62. Cartier, N. *et al.* Hematopoietic stem cell gene therapy with a lentiviral vector in X-linked adrenoleukodystrophy. *Science* **326**, 818–823 (2009).
63. Biti, R. *et al.* HIV-1 infection in an individual homozygous for the CCR5 deletion allele. *Nat. Med.* **3**, 252–253 (1997).
64. Oh, D.Y. *et al.* CCR5Delta32 genotypes in a German HIV-1 seroconverter cohort and report of HIV-1 infection in a CCR5Delta32 homozygous individual. *PLoS ONE* **3**, e2747–2753 (2008).
65. Weiser, B. *et al.* HIV-1 coreceptor usage and CXCR4-specific viral load predict clinical disease progression during combination antiretroviral therapy. *AIDS* **22**, 469–479 (2008).
66. Ogert, R.A. *et al.* Mapping Resistance to the CCR5 co-receptor antagonist vicriviroc using heterologous chimeric HIV-1 envelope genes reveals key determinants in the C2–V5 domain of gp120. *Virology* **373**, 387–399 (2008).
67. Soulie, C. *et al.* Primary genotypic resistance of HIV-1 to CCR5 antagonist treatment-naïve patients. *AIDS* **22**, 2212–2214 (2008).
68. Palmer, S. *et al.* Low-level viremia persists for at least 7 years in patients on suppressive antiretroviral therapy. *Proc. Natl. Acad. Sci. USA* **105**, 3879–3884 (2008).
69. Dinoso, J.B. *et al.* Treatment intensification does not reduce residual HIV-1 viremia in patients on highly active antiretroviral therapy. *Proc. Natl. Acad. Sci. USA* **106**, 9403–9408 (2009).
70. Mitsuyasu, R.T. *et al.* Phase 2 gene therapy trial of an anti-HIV ribozyme in autologous CD34+ cells. *Nat. Med.* **15**, 285–292 (2009).

## ONLINE METHODS

**Hematopoietic stem/progenitor cell isolation.** Human CD3<sup>+</sup> HSPCs were isolated from umbilical cord blood collected from normal deliveries at local hospitals, according to guidelines approved by the Children's Hospital Los Angeles Committee on Clinical Investigation, or as waste cord blood material from StemCyte Corp. Immunomagnetic enrichment for CD34<sup>+</sup> cells was performed using the magnetic-activated cell sorting (MACS) system (Miltenyi Biotec), per the manufacturer's instructions, with the modification that the initial purified CD34<sup>+</sup> population was put through a second column and washed three times with 3 ml of the supplied buffer per wash before the final elution. This additional step gave a > 99% pure CD34<sup>+</sup> population, as measured by FACS analysis using the anti-CD34 antibody, 8G12 (BD Biosciences).

**Nucleofection of CD34<sup>+</sup> HSPCs with ZFN expression plasmids.** Freshly isolated CD34<sup>+</sup> cells were stimulated for 5–12 h in X-VIVO 10 media (Lonza) containing 2 nM L-glutamine, 50 ng/ml SCF, 50 ng/ml Flt-3 and 50 ng/ml TPO (R&D Systems). 1 × 10<sup>6</sup> cells were nucleofected with 2.5 µg each of a plasmid pair expressing ZFNs binding upstream (ZFN-L) or downstream (ZFN-R) of codon Leu55 within TM1 of human *CCR5* (ref. 19). The CD34<sup>+</sup> cell/DNA mix was processed in an X series Amaxa Nucleofector (Lonza) using the U-01 setting and the human CD34<sup>+</sup> nucleofector solution, according to the manufacturer's instructions. Following nucleofection, cells were immediately placed in pre-warmed IMDM media (Lonza) containing 26% FBS (Mediatech), 0.35% BSA, 2nM L-glutamine, 0.5% 10<sup>-3</sup> mol/l hydrocortisone (Stem Cell Technologies), 5 ng/ml IL-3, 10 ng/ml IL-6 and 25 ng/ml SCF (R&D Systems). Cells were allowed to recover in this media for 2–12 h before injection into mice.

**Apoptosis assay.** CD34<sup>+</sup> HSPCs were collected at 24 h post-nucleofection and analyzed for the percent of viable cells marked for apoptosis using the PE apoptosis detection kit (BD Biosciences) according to the manufacturer's instructions. Cells were stained with 7-AAD (detects viable cells) and annexin V (detects apoptotic cells) and analyzed using a FACScan flow cytometer (BD Biosciences). This double staining allowed the identification of cells in the early stages of apoptosis.

**NSG mouse transplantation.** NOD.Cg-Prkdc scid Il2rg tm1Wj/SzJ (NOD/SCID/IL2r<sup>γ</sup>null, NSG) mice<sup>71</sup> were obtained from Jackson Laboratories. Neonatal mice within 48 h of birth received 150 cGy radiation, then 2–4 h later 1 × 10<sup>6</sup> ZFN-modified or mock-treated human CD34<sup>+</sup> HSPCs in 50 µl PBS containing 1% heparin were injected through the facial vein. For secondary transplantations, bone marrow was harvested by needle aspiration from the upper and lower limbs of 18-week-old animals previously engrafted with human CD34<sup>+</sup> HSPCs, filtered through a 70 µm nylon mesh screen (Fisher Scientific) and washed in PBS. The cells were transplanted into three 8-week-old mice that had previously received 350 cGy radiation, using retro-orbital injection of 2 × 10<sup>7</sup> bone marrow cells per mouse. Mouse cohorts are described in **Supplementary Table 2**.

**Analysis of *CCR5* disruption.** The percentage of *CCR5* alleles disrupted by ZFN treatment was measured by performing PCR across the ZFN target site followed by digestion with the Surveyor (Cel 1) nuclease (Transgenomic), which detects heteroduplex formation, as previously described<sup>19</sup>. Briefly, genomic DNA was extracted from mouse tissues and subject to nested PCR amplification using human *CCR5*-specific primers, with the resulting radiolabeled products digested with Cel 1 nuclease and resolved by PAGE. The ratio of cleaved to uncleaved products was calculated to give a measure of the frequency of gene disruption. The assay is sensitive enough to detect single-nucleotide changes and has a linear detection range between 0.69 and 44%<sup>19</sup>.

In addition, a common 5-bp (pentamer) duplication that occurs after nonhomologous end-joining repair of ZFN-cleaved *CCR5* (ref. 19) was detected by PCR. The first-round PCR product generated during Cel 1 analysis was diluted 1:5,000 and 5 µl used in a Taqman qPCR reaction using primers (5'-GGTCATCCTCATCCTGATCTGA-3' and 5'-GATGATGAAGAAGATTCCAGAGAAGAAG-3') and probe 5'-FAM d

(CCTTCTTACTGTCCCTTCTGGGCTCAC) BHQ-1-3' (Biosearch Technologies), and analyzed using a 7,900HT real-time PCR machine (Applied Biosystems). At the same time, 5 µl of a 1:50,000 dilution of the PCR product were used in a Taqman qPCR reaction using primers (5'-CCAAAAATCAATGTGAAGCAAATC-3' and 5'-TGCCACAAAACCAAAGATG-3') and probe 5'-FAM d(CAGCCGCCTCCTGCCTCC) BHQ-1-3' to detect total copies of human *CCR5*. Data were analyzed using software supplied by the manufacturer and the frequency of pentamer insertions in *CCR5* calculated. The assay is sensitive enough to detect a single pentamer insertion event in 100,000 cells (data not shown).

ZFN-induced modifications of *CCR5* were analyzed by directly sequencing cloned *CCR5* alleles, isolated by PCR amplification as described above, and TOPO-TA cloning (Invitrogen). Plasmid DNA was isolated from 60 individual bacterial colonies for each tissue analyzed.

**HIV-1 infection and analysis.** A cell-free virus stock of HIV-1<sub>BaL</sub> and a molecular clone of HIV-1<sub>NL4-3</sub> were obtained from the AIDS Research and Reference Reagent Program (ARRRP), Division of AIDS, NIAID, NIH from material deposited by Suzanne Gartner, Mikulas Popovic, Robert Gallo and Malcolm Martin. HIV-1<sub>BaL</sub> virus was propagated in PM1 cells, obtained from the ARRRP and deposited by Marvin Reitz and harvested 10 d post-infection. HIV-1<sub>NL4-3</sub> viruses were generated by transient transfection of 293T cells (ATCC). Viruses were titrated using the Alliance HIV-1 p24 ELISA kit (PerkinElmer) and by TCID<sub>50</sub> analysis on U373-MAGI cells (ARRRP, deposited by Michael Emerman and Adam Geballe). Mice to be infected with HIV-1 were anesthetized with inhalant 2.5% isoflourane and injected intraperitoneally with virus stocks containing 200 ng p24, 7 × 10<sup>4</sup> TCID<sub>50</sub> units, in 100 µl total volume.

HIV-1 levels in peripheral blood or tissues harvested at necropsy were determined by extracting RNA from 5 × 10<sup>5</sup> cells using the master pure complete DNA and RNA purification kit (Epicentre Biotechnologies) and performing Taqman qPCR using a primer and probe set targeting the HIV-1 LTR region, as previously described<sup>72</sup>. In addition, p24 levels were measured in blood samples by ELISA.

**Mouse blood and tissue collection.** Peripheral blood samples were collected every 2 weeks starting at 8 weeks of age, using retro-orbital sampling. Whole blood was blocked in FBS (Mediatech) for 30 min., the red blood cells were lysed using Pharmlyse solution (BD Biosciences) and cells were washed with PBS. Tissue samples were collected at necropsy and processed immediately for cell isolation and FACS analysis, or kept in freezing media (IMDM plus 20% DMSO) in liquid nitrogen, for later analysis and DNA extraction. Tissue samples were manually agitated in PBS before filtering through a sterile 70 µm nylon mesh screen (Fisher Scientific) and suspension cell preparations produced as previously described<sup>19</sup>. Intestinal samples were processed as previously described<sup>73</sup>, with the modification that the mononuclear cell population was isolated after incubation in citrate buffer and collagenase enzyme for 2 h, followed by nylon wool filtration (Amersham Biosciences) and ficoll-hypaque gradient isolation (GE Healthcare).

**Analysis of human cells in mouse tissues.** FACS analysis of human cells was performed using a FACSCalibur instrument (BD Biosciences) with either BD CellQuest Pro version 5.2 (BD Biosciences) or FlowJo software version 8.8.6 for Macintosh (Treestar). The gating strategy performed was an initial forward scatter versus side scatter (FSC/SSC) gate to exclude debris, followed by a human CD45 gate. For analysis of lymphocyte populations in peripheral blood, a further lymphoid gate (low side scatter) was also applied to exclude cells of monocytic origin<sup>74</sup>. All antibodies used were fluorochrome conjugated and human specific, and obtained from BD Biosciences: CD45 (clone 2D1), CD19 (clone HIB19), CD14 (clone MØP9), CD3 (clone SK7), CD4 (clone SK3), CD8 (clone HIT8a), *CCR5* (2D7). Gates were set using fluorescence minus one controls, where cells were stained with all antibodies except the one of interest. Specificity was also confirmed using isotype-matched nonspecific antibodies (BD Biosciences) (**Supplementary Fig. 1**) and with tissues from animals that had not been engrafted with human cells.

Immunohistochemical analysis of human CD3 and CD4 expression, respectively, in the small intestine and spleen tissue from HSPC-engrafted

mice was performed on fixed paraffin-embedded tissue sections, as previously described<sup>73</sup>. Controls included isotype-matched nonspecific antibodies and unengrafted NSG mice.

**Statistical analysis.** All statistical analysis was performed using GraphPad Prism version 5.0b for Mac OSX (GraphPad Software). Unpaired two-tailed *t*-tests were performed assuming equal variance to calculate *P*-values. A 95% confidence interval was used to determine significance. A minimum of three data points was used for each analysis.

71. Shultz, L.D. *et al.* Human lymphoid and myeloid cell development in NOD/LtSz-scid IL2R gamma null mice engrafted with mobilized human hematopoietic stem cells. *J. Immunol.* **174**, 6477–6489 (2005).
72. Rouet, F. *et al.* Transfer and evaluation of an automated, low-cost real-time reverse transcription-PCR test for diagnosis and monitoring of human immunodeficiency virus type 1 infection in a West African resource-limited setting. *J. Clin. Microbiol.* **43**, 2709–2717 (2005).
73. Sun, Z. *et al.* Intrarectal transmission, systemic infection, and CD4+ T cell depletion in humanized mice infected with HIV-1. *J. Exp. Med.* **204**, 705–714 (2007).
74. Loken, M.R. *et al.* Establishing lymphocyte gates for immunophenotyping by flow cytometry. *Cytometry* **11**, 453–459 (1990).